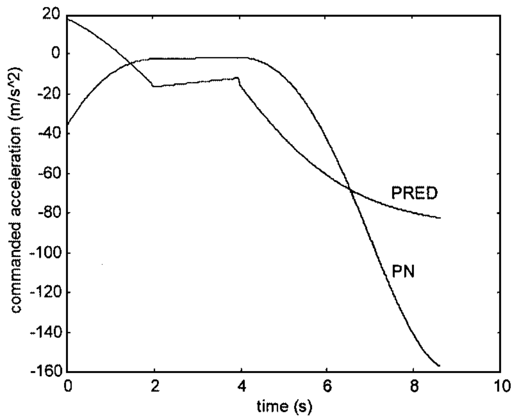

Fig. 2 Commanded acceleration profiles.

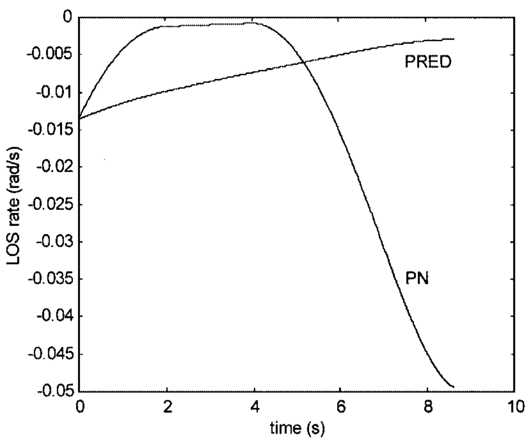

Fig. 3 LOS rate profiles.

Conclusion

In this Note, a new formulation of PNG is derived based on the recently developed continuous-time predictive control approach. Simulations have been carried out to assess the performance of this guidance law in comparison with conventional PNG for a maneuvering target, and results are presented. The results show that the present guidance law gives superior performance compared with the conventional PNG law.

Acknowledgments

The first author acknowledges S. B. Phadke, G. C. Pant, Chairman of the Faculty of Guided Missiles, and G. S. Mani, Director and Dean of the Institute of Armament Technology, for providing motivation and support during the course of this work.

References

[1]Lu, P., "Optimal Predictive Control of Continuous Nonlinear Systems," *International Journal of Control*, Vol. 62, No. 3, 1995, pp. 633–649.

[2]Singh, S. N., Steinberg, M., and DiGirolamo, R. D., "Nonlinear Predictive Control of Feedback Linearizable Systems and Flight Control System Design," *Journal of Guidance, Control, and Dynamics*, Vol. 18, No. 5, 1995, pp. 1023–1028.

[3]Nijmeijer, H., and Van Der Shaft, A. J., *Nonlinear Dynamical Control Systems*, Springer–Verlag, New York, 1990, pp. 72, 73.

[4]Bezick, S., Rusnak, I., and Grey, W. S., "Guidance of a Homing Missile via Nonlinear Geometric Control Methods," *Journal of Guidance, Control, and Dynamics*, Vol. 18, No. 3, 1995, pp. 441–448.

[5]Ha, I. J., Hur, J. S., Ko, M. S., and Song, T. L., "Performance of PNG Laws for Randomly Maneuvering Targets," *IEEE Transactions on Aerospace and Electronic Systems*, Vol. 26, No. 5, 1990, pp. 713–720.

[6]Babu, K. R., Sarma, I. G. S., and Swamy, K. N., "Switched Biased Proportional Navigation for Homing Guidance Against Highly Maneuvering Targets," *Journal of Guidance, Control, and Dynamics*, Vol. 17, No. 6, 1994, pp. 1357–1363.

Guidance Strategy for Solid Propelled Launchers

Waldemar de Castro Leite Filho*
and Pelson de Souza Pinto†
Instituto de Aeronáutica e Espaço,
12228-904 Sao José dos Campos, Brazil

Introduction

THIS Note describes the guidance strategy used for the Brazilian satellite launcher,[1] called VLS. The vehicle has four stages and uses solid fuel; the last stage is spin stabilized. Its first mission was to place a 115-kg satellite into a 750-km altitude circular orbit. Because there is no velocity control—the burning of the fourth stage cannot be interrupted—the final orbit is determined by the suborbital trajectory (ballistic phase) between the third and fourth stages, the ignition time of the fourth stage, and its inertial attitude. Thus, to achieve the prescribed altitude of a circular orbit, the last stage must be in a particular ballistic trajectory and the last action of the control system is to point the fourth-stage/satellite assembly to a certain inertial direction and to decide the ignition time.

The guidance commands produce, during the third stage, the reference to the attitude control system so that the vehicle reaches a transfer orbit with prespecified parameters, called parametric suborbit guidance (PSG). Regarding the fourth stage, the guidance command sets the inertial direction and establishes the ignition time. This is called the pointing algorithm (PA).

Pointing Algorithm

The PA[2,3] calculates the ignition time and the inertial attitude for the fourth stage based on real navigation data to obtain a proper transfer to a circular orbit. The strategy should operate during the coast phase between the third-stage burnout and the fourth-stage ignition. The strategy proposed is similar to an impulsive orbit transfer because the fourth-stage energy is considered as an increment of velocity. The main difference to the impulsive assumption is the ignition time. The real ignition time has an additional term that is obtained based on conservation of energy. After this, the obtained deployment attitude[4] is related to the inertial frame. The algorithm assumes that no disturbance is present during the coast phase to change that Keplerian orbit.

During the coast phase and the burning of the last stage, the equation of motion of the vehicle center of mass[4] is $\ddot{\boldsymbol{R}} = g(\boldsymbol{R}) + \Gamma(t) \cdot \boldsymbol{\vartheta}$, where $\boldsymbol{R}$ is the vehicle radius vector, g is the gravitational acceleration, $\boldsymbol{\vartheta}$ is a constant unit vector in the thrust direction (kept constant by the attitude control system), and $\Gamma(t)$ is the propulsive acceleration that is assumed to be a well-known function. The solution of $\boldsymbol{R}(t)$ can be formulated as

$$\boldsymbol{V} = V_0 + \Delta V \cdot \vartheta + \Delta \boldsymbol{V}_g$$

$$R = R_0 + (t - t_0) \cdot \boldsymbol{V}_0 + \Delta R \cdot \vartheta + \Delta \boldsymbol{R}_g$$

where

$$\Delta \boldsymbol{V}_g = \int_{t_0}^{t} \frac{\mu \boldsymbol{R}(\xi)}{R(\xi)^3}\, \mathrm{d}\xi, \qquad \Delta V = \int_{t_{ig}}^{t} \Gamma(\xi)\, \mathrm{d}\xi$$

t_{ig} is the ignition time with $t_0 \le t_{ig}$, and ΔR and $\Delta \boldsymbol{R}_g$ are, respectively, the integration of ΔV and $\Delta \boldsymbol{V}_g$.

The increment of angular momentum over the last stage is given by $\Delta \boldsymbol{H} = \boldsymbol{R} \times m \cdot \boldsymbol{V} - \boldsymbol{R}_0 \times m_0 \cdot \boldsymbol{V}_0$. The motion is considered to

Received Dec. 29, 1997; revision received July 13, 1998; accepted for publication July 20, 1998.

*Senior Researcher, Space Systems Division, Praca Marechal Eduardo Gomes 50. Associate Member AIAA.

†Senior Researcher, Space Systems Division, Praca Marechal Eduardo Gomes 50.

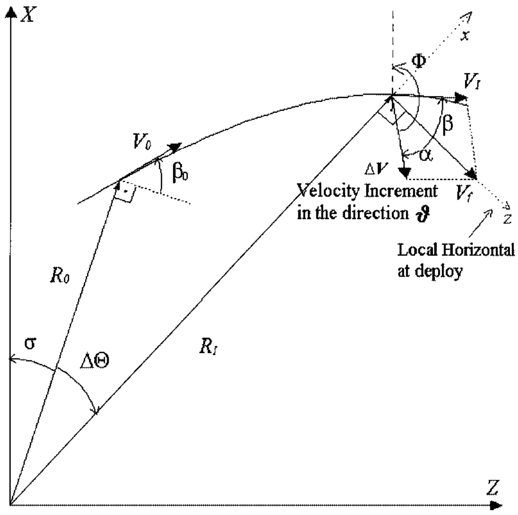

Fig. 1 Vector diagram in the impulsive shot.

take place in a limited region of space, resulting in a small arc. Therefore, the gravity loss $\Delta\boldsymbol{R}_g$ has nearly the same direction of $\boldsymbol{R}_0$ and $\Delta\boldsymbol{R}_g \approx (t_f - t_{\text{ig}}) \cdot \Delta\boldsymbol{V}_g$, where t_f is the fourth-stage burnout time.[4] This idealization is generally acceptable when the distance traveled during a propelled phase is negligible when compared with the radius vector. It follows that the terms $\Delta\boldsymbol{R}_g \times \boldsymbol{V}_0$, $\boldsymbol{R}_0 \times \Delta\boldsymbol{V}_g$, $\boldsymbol{V}_0 \times \Delta\boldsymbol{V}_g$, and $\Delta\boldsymbol{R}_g \times \Delta\boldsymbol{V}_g$ are null. These simplifications yield

$$\Delta\boldsymbol{H} = m\{\boldsymbol{R}_0 + [(t_f - t_{\text{ig}}) - \Delta R/\Delta V] \cdot [\boldsymbol{V}_0 + \boldsymbol{V}_g]\} \times \Delta V \cdot \boldsymbol{\vartheta} + (m - m_0) \cdot \boldsymbol{R}_0 \times \boldsymbol{V}_0$$

which can be rewritten as

$$\Delta\boldsymbol{H} = m\boldsymbol{R}_I \times [\boldsymbol{V}_I + \Delta V \cdot \boldsymbol{\vartheta}] - m_0 \cdot \boldsymbol{R}_I \times \boldsymbol{V}_I$$

where $\boldsymbol{R}_I = \boldsymbol{R}_0 + [(t_f - t_{\text{ig}}) - \Delta R/\Delta V] \cdot [\boldsymbol{V}_0 + \boldsymbol{V}_g]$. It can be observed that the expression of $\Delta\boldsymbol{H}$ is equivalent to an orbital change due to impulsive thrust applied in $\boldsymbol{R}_I$ because in a Keplerian orbit $\boldsymbol{R}_0 \times \boldsymbol{V}_0 = \boldsymbol{R}_I \times \boldsymbol{V}_I$. This conclusion means that the actual thrust started in t_{ig} at the fixed direction $\boldsymbol{\vartheta}$ and the impulsive shot in $\boldsymbol{R}_I$ with the same direction have equivalent results. Besides, R_I will be reached η seconds after the ignition time t_{ig}, where $\eta = (t_f - t_{\text{ig}}) - \Delta R/\Delta V$. Then it is acceptable to say that η is a correction factor of the impulsive time ignition t_I ($\eta \approx 42.3$ s), and so it will have the same effect of an actual thrust with $t_{\text{ig}} = t_I - \eta$.

Figure 1 shows the conditions for $\boldsymbol{V}$, at the instant t_I, to be added by a velocity increment $\Delta\boldsymbol{V}$ to reach a circular orbit. The circular orbit has the final velocity $V_f = \sqrt{(\mu/R)}$, and the conditions to find V_f are

$$V \cdot \sin(\beta) = -\Delta V \cdot \sin(\alpha) \tag{1}$$

$$V \cdot \cos(\beta) + \Delta V \cdot \cos(\alpha) = \sqrt{\mu/R} \tag{2}$$

The Keplerian orbit yields

$$V^2 - 2\mu/R = V_0^2 - 2\mu/R_0 = -\mu/a \tag{3}$$

$$V \cdot R \cdot \cos(\beta) = V_0 \cdot R_0 \cdot \cos(\beta_0) \tag{4}$$

where a is the semimajor axis of the ascent trajectory. Equations (1–4) can be expressed as

$$\Delta V^2 + \mu/a - \mu/R = 2\Delta V \cos(\alpha)\sqrt{\mu/R} \tag{5}$$

$$R\left[\sqrt{\mu/R} - \Delta V \cos(\alpha)\right] = V_0 R_0 \cos(\beta_0) \tag{6}$$

Substitution of Eq. (6) into Eq. (5) yields

$$\sqrt{R}\left[\frac{3}{2} - R\left(\frac{\Delta V^2}{2\mu} + \frac{1}{2a}\right)\right] = \frac{V_0 R_0 \cos(\beta_0)}{\sqrt{\mu}} \tag{7}$$

where $\beta_0 = \arcsin(\boldsymbol{R} \circ \boldsymbol{V}/(R \cdot V))$.

Equation (7) can be considered a third-order polynomial with $\sqrt{R}$ as its variable. It has a practical analytical solution because the second-order term vanished:

$$R_I = \frac{4\cos^2(\lambda/3 + 2\pi/3)}{\Delta V^2/\mu + 1/a} \tag{8}$$

where $\lambda = \arccos[V_0 R_0 \cos(\beta_0)\sqrt{(\Delta V^2/\mu + 1/a)}/\sqrt{\mu}]$.

Equation (5) yields

$$\alpha = \arccos\left\{\frac{\sqrt{R_I/\mu}\left[\Delta V^2 + \mu(1/a - 1/R_I)\right]}{2\Delta V}\right\} \tag{9}$$

Equations (8) and (9) express the value of the circular orbit radius of the vehicle after the burnout of the last stage, with the deployment angle α. This angle must be represented in the inertial attitude for the vehicle to be in the correct orientation.

The equivalent impulsive burn time t_I is relative to the period of time the vehicle takes to move from R_0 to R_I. It can be expressed in terms of the eccentric anomaly E by

$$\sqrt{\mu/a^3} \cdot (t_I - t_0) = E_I - E_0 - e \cdot [\sin(E_I) - \sin(E_0)] \tag{10}$$

where

$$E = \arccos[(a - R)/(a \cdot e)]$$

and where

$$e^2 = [(RV^2/\mu) - 1]^2 \cos^2(\beta) + \sin^2(\beta)$$

is the ascent trajectory eccentricity. According to Eq. (10), the true time ignition t_{ig} can be obtained by

$$t_{\text{ig}} = \sqrt{a^3/\mu} \cdot [(E_I - E_0) - e(\sin(E_I) - \sin(E_0))] + \Delta R/\Delta V - \tau + t_0$$

where $\tau = (t_f - t_{\text{ig}})$ is the burn time of the last stage ($\tau \approx 70$ s).

The results obtained are relative to the flight plane. The pitch angle Φ, relative to this plane, can be expressed (see Fig. 1) as $\Phi = -\pi/2 + \sigma - \Delta\Theta - \alpha$, where σ is the pitch angle of $\boldsymbol{R}_0$ and $\Delta\Theta$ is the difference of the eccentric anomaly. To express this angle in the navigational frame it is necessary, first, to find the relation between the flight plane and the navigational frame. The orientation of the trajectory plane is defined by two angles, the right ascension of the ascending node Ω and the inclination i given by $\cos(i) = (\boldsymbol{u}_y \circ \boldsymbol{D})/D = D_y/D$, where $\boldsymbol{D} = \boldsymbol{V} \times \boldsymbol{R}$, and $\tan(\Omega) = -D_z/D_x$. This relation permits the transformation of the pitch angle, from the flight plane coordinates to the navigational frame, in terms of the Euler angles $\theta_p = -\pi + \arctan(-T_z/T_x)$ and $\psi_p = \arcsin(T_y)$, where

$$T_x = \cos(i)\cos(\Omega)\cos(\Phi) - \sin(\Omega)\sin(\Phi)$$

$$T_y = \sin(i)\cos(\Phi)$$

$$T_z = -\cos(i)\sin(\Omega)\cos(\Phi) - \cos(\Omega)\sin(\Phi)$$

The angles θ_p and ψ_p define the direction $\boldsymbol{\vartheta}$ where the last stage must be pointed at the instant t_{ig}. Then the vehicle will be transferred to a circular orbit with radius R_I. Therefore, the pointing algorithm, based on the position and velocity inertial data, looks for the possible circular orbit that the vehicle can reach, independent of its radius.

The algorithm described earlier assumes that the orbit injection will take place in the same plane of the orbit of the last stage ballistic phase (before its ignition). However, it is possible to change this algorithm[5] to allow the orbit injection into a different orbital plane. With this improvement the pointing algorithm becomes more general. It can be used not only to obtain a circular orbit, but also to change the orbit inclination, provided the impulsive increment of velocity assures sufficient energy to fulfill both tasks.

Parametric Suborbit Guidance

The equivalence between the actual thrust started in t_{ig} at the fixed direction ϑ and the impulsive shot in $\boldsymbol{R}_I$ with same direction allows the evaluation of the velocity after the last stage burnout ($\boldsymbol{V}$) through a vectorial sum of the velocity just before the last stage ignition ($\boldsymbol{V}_0$) with the velocity increment due to its complete burning ($\Delta\boldsymbol{V}$). Given an orbital radius R, the set of equations (1–4) permits the consideration of the problem at the end of third stage, resulting in a set of four equations with six variables. This set of equations defines a family of suborbital trajectories, which satisfies both conditions at the end of the third stage (R_0, V_0, and β_0) and the conditions for the ignition of the fourth stage (R_I, V_I, β_I, and α). Algebraic manipulation leads to the following relationship:

$$\cos\beta_0 = \frac{R_{\text{sat}}}{2\sqrt{(\mu/R_{\text{sat}})}\cdot V_0\cdot R_0} \times\left[V_0^2 + 2\mu\cdot\left(\frac{1}{R_{\text{sat}}}-\frac{1}{R_0}\right)+\frac{\mu}{R_{\text{sat}}}-\Delta V^2\right] \tag{11}$$

where R_{sat} is the same R_I stated before; however, in this case R_{sat} is a parameter (from the orbit specification), whereas in the pointing algorithm R_I is the independent variable of the equations. Therefore, Eq. (11) defines the target subspace for the third-stage guidance. The guidance problem was solved in a particular frame, hereafter called the guidance frame (see Fig. 1), that is defined as follows: the x axis aligns with the position vector, the y axis is orthogonal to the plane spanned by the position and velocity vectors, and the z axis completes the right-hand frame.

The frame transformations are easily derived, and with some additional simplifications that will be explained later, the equations of motion of the third stage are derived as follows:

$$\frac{dV_x}{dt} = \Gamma_3(t)\cdot\cos(\alpha_3+\omega t)\cos(\varphi_3)$$

$$\frac{dV_z}{dt} = \Gamma_3(t)\cdot\sin(\alpha_3+\omega t)\cos(\varphi_3) - g \tag{12}$$

$$\frac{dV_y}{dt} = \Gamma_3(t)\cdot\sin(\varphi_3), \qquad \frac{d\boldsymbol{R}}{dt} = \boldsymbol{V}(t)$$

where α_3 and φ_3 are the deployment attitude and $\Gamma_3(t)$ is the third-stage propulsive acceleration, which is known, from the actual time t_a until the burnout of the third stage t_{bo}.

One hypothesis that simplifies this problem (which, in fact, imposes the control law) is that the deployment attitude α_3 is calculated by $\alpha_3(t) = \alpha_a(t) + \omega\cdot t$. The other hypotheses are that the parameter ω is considered constant during the remaining time of the third stage and that the guidance frame is frozen. Then, Eqs. (12) could be integrated (even analytically), and as a result, the conditions at the burnout of the third stage (t_{bo}, R_{bo}, and V_{bo}) can be estimated. Hence, given the information of the actual time $\boldsymbol{R}_a$ and $\boldsymbol{V}_a$ and considering the available energy (from the actual time till the burnout), it is possible to estimate where the vehicle will go for a given ω. It follows that the flight-path angle β_0 at that point can also be calculated, and it is, of course, a function of ω. Therefore, to solve the guidance problem it is necessary to find the value of ω that makes the solution of Eqs. (12) reach the desired flight-path angle β_0, the velocity V_0,

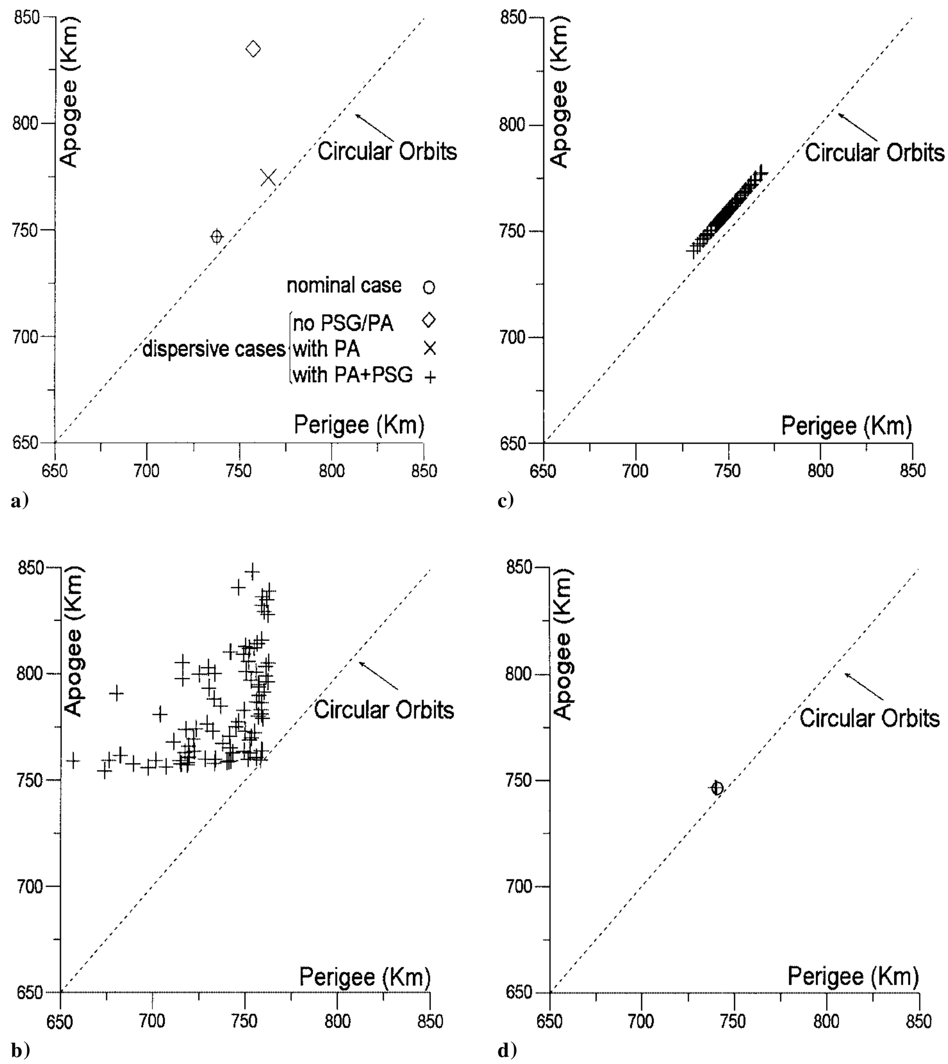

Fig. 2 Final orbits obtained with Monte Carlo study.

and the position R_0 solving Eq. (11). This process results in the following set of four equations and four variables (ω, β_0, V_0, and R_0):

$$R_0 = |\boldsymbol{R}(t_{bo}, t_a, \omega)|, \qquad V_0 = |\boldsymbol{V}(t_{bo}, t_a, \omega)|$$

$$\beta_0 = \arcsin\left[\frac{\boldsymbol{R}_{bo} \circ \boldsymbol{V}_{bo}}{(R_{bo} \cdot V_{bo})}\right]$$

$$\cos\beta_0 = \frac{R_{sat}}{2\sqrt{(\mu/R_{sat})} \cdot V_0 \cdot R_0}\left[V_0^2 + 2\mu \cdot \left(\frac{1}{R_{sat}} - \frac{1}{R_0}\right) + \frac{\mu}{R_{sat}} - \Delta V^2\right]$$

To have a closed-loop solution, ω is calculated periodically. The period was chosen as a compromise between onboard-computer load and algorithm accuracy. The value of 1 s was used in the present study. During this interval, the reference attitude was calculated by $\alpha_{3k+1} = \alpha_{3k} + \omega_k \cdot \delta t$, where δt is the onboard-computer sample interval, and the necessary frame transformation is made to get the Euler angles θ_r and ψ_r to be the reference for the attitude control system (the same transformation that is used in the pointing algorithm).

Results

To assess the performance of the guidance strategies (PA and PSG), digital simulations were done. The simulation program included most of the known nonlinearities (e.g., nonspherical Earth effects). A Monte Carlo simulation was performed, and the results were compared with the nominal trajectory without disturbances. Figure 2a shows the differences of the final orbit when no guidance was used, when only the PA algorithm was used, and when both PA and PSG algorithms were used, in the presence of a dispersion of 10% in the drag coefficient. Figure 2b shows the results of a Monte Carlo flight simulation without the PSG and the PA algorithms, which considered the random choice of the thrust profile ($3\sigma = 2\%$ of impulse) of the first and second stages, the vehicle mass ($3\sigma = 0.5\%$), the drag coefficient ($3\sigma = 10\%$), and the attitude misalignment ($3\sigma = 1$ deg) of the last stage (to orbit injection). Figure 2c shows the results of the same simulation when only the PA algorithm was included, and Fig. 2d shows the results when both the PA and the PSG algorithms were included. When both guidance strategies were used, the final orbits are so close that it is not possible to distinguish them, showing the validity of the hypotheses made.

Conclusions

The simulation results have shown that the guidance strategies PSG connected to PA fulfill an important reduction in the dispersion of the orbit parameters, resulting from errors of the first and second stages' thrust, the drag coefficient, and the pointing angle. Besides the good results in the performance, the proposed strategies have the following advantages:

1) Their algorithms are simple and easy to implement in the onboard computer.

2) The PSG algorithm can be started at any time during the burning of the third stage without any discontinuity in the attitude command (because the PSG output is the angular velocity).

3) Both strategies are suitable for solid propellant engines.

4) The PSG algorithm can set alternate altitudes if the evaluated energy is not enough to reach the nominal one.

The disadvantages detected are the following:

1) Using these strategies, it is not possible to control directly the velocity magnitude. Energy control is possible only by changing the attitude.

2) The calculation is based on an estimate of the energy available in the subsequent stages.

These results are the main reason that led the control system team to choose the PSG and the PA algorithms as the main guidance loop for the first flight of the Brazilian VLS.

References

[1] Yoshino, T., Boscov, J., and Shimote, W. K., "Main Propulsion System of Brazilian Satellite Launch Vehicle VLS," *Proceedings of the 16th International Symposium on Space Technology and Science*, Inst. of Space and Astronautical Science, Sapporo, Japan, 1988, pp. 149–155.

[2] Malyshev, V. V., Krasilshikov, M. N., Bobronnikov, V. T., Dishel, V. D., Leite Filho, W. C., and Ribeiro, T. S., "Launcher Guidance Algorithm Design," *Aerospace Vehicle Control: Modern Theory and Applications*, Inst. de Aeronáutica e Espaço, Sao José dos Campos, Brazil, 1996, pp. 303–344.

[3] Leite Filho, W. C., "Pointing Algorithm: A Strategy for Orbit Injection with Uncontrolled Last Stage," *Proceedings of the 2nd ESA International Conference on Spacecraft Guidance, Navigation, and Control Systems*, European Space Research and Technology Centre, Noordwijk, The Netherlands, 1994, pp. 339–342.

[4] Regan, F. J., and Anandakrishnan, S. M., "Keplerian Motion," *Dynamic of Atmospheric Reentry*, AIAA, Washington, DC, 1993, pp. 145–177.

[5] Leite Filho, W. C., "Strategies for Orbit Injection That Includes Yaw Maneuver," *Proceedings of the 3rd ESA International Conference on Spacecraft Guidance, Navigation, and Control Systems*, European Space Research and Technology Centre, Noordwijk, The Netherlands, 1996, pp. 657–659.

Gain-Weighted Eigenspace Assignment

John B. Davidson Jr.*
NASA Langley Research Center, Hampton, Virginia 23681
and
Dominick Andrisani II†
Purdue University, West Lafayette, Indiana 47907

Introduction

A DIRECT eigenspace assignment method[1–4] has been used to design lateral-directional control laws for NASA's High Angle-of-Attack Research Vehicle.[5] The control laws developed have demonstrated good performance, robustness, and flying qualities during both piloted simulation and flight testing. During the control-law design effort, a limitation of the direct eigenspace assignment method became apparent—the designer has no direct control over feedback-gain magnitudes. The development of an eigenspace (eigenstructure) assignment method[6] that overcomes this limitation is presented.

Gain-Weighted Eigenspace Assignment Methodology

For a system that is observable and controllable and has n states, m controls, and l measurements, this method allows a designer to place l eigenvalues at desired locations and trade off the achievement of desired eigenvectors vs feedback-gain magnitudes. The following development assumes that complex matrices have been converted to real Jordan form. Given the observable, controllable system

$$\dot{x} = Ax + Bu \tag{1}$$

where $x \in \boldsymbol{R}^n$ and $u \in \boldsymbol{R}^m$, with system measurements available for feedback given by

$$z = Mx + Nu \tag{2}$$

where $z \in \boldsymbol{R}^l$. The total control input is the sum of the augmentation input u_c and pilot's input u_p

$$u = u_p + u_c \tag{3}$$

The measurement feedback-control law is

$$u_c = Gz \tag{4}$$

Received June 17, 1997; revision received April 20, 1998; accepted for publication May 7, 1998.

*Aerospace Engineer, Mail Stop 132. Senior Member AIAA.

†Associate Professor, School of Aeronautics and Astronautics. Senior Member AIAA.